Int J Legal Med (2007) 121: 9–17
DOI 10.1007/s00414-005-0058-6

ORIGINAL ARTICLE

S. A. Blackwell · R. V. Taylor · I. Gordon · C. L. Ogleby · T. Tanijiri · M. Yoshino · M. R. Donald · J. G. Clement

3-D imaging and quantitative comparison of human dentitions and simulated bite marks

Received: 7 August 2005 / Accepted: 13 October 2005 / Published online: 4 January 2006

Abstract This study presents a technique developed for 3-D imaging and quantitative comparison of human dentitions and simulated bite marks. A sample of 42 study models and the corresponding bites, made by the same subjects in acrylic dental wax, were digitised by laser scanning. This technique allows image comparison of a 3-D dentition with a 3-D bite mark, eliminating distortion due to perspective as experienced in conventional photography. Cartesian co-ordinates of a series of landmarks were used to describe the dentitions and bite marks, and a matrix was created to compare all possible combinations of matches and non-matches using cross-validation techniques. An algorithm, which estimated the probability of a dentition matching its corresponding bite mark, was developed. A receiver operating characteristic graph illustrated the relationship between values for specificity and sensitivity. This graph also showed for this sample that 15% of non-matches could not be distinguished from the true match, translating to a 15% probability of falsely convicting an innocent person.

Keywords Forensic odontology · Bite mark · 3-dimensional · 3-D quantification · Animation

S. A. Blackwell (✉) · R. V. Taylor · J. G. Clement
Oral Anatomy, Medicine and Surgery Unit,
School of Dental Science, Faculty of Medicine,
Dentistry and Health Sciences,
The University of Melbourne,
720 Swanston Street,
3010, Victoria, Australia,
e-mail: sherie@unimelb.edu.au
Fax: +61-3-93411594

I. Gordon · M. R. Donald
Statistical Consulting Centre,
The University of Melbourne,
3010, Victoria, Australia,

C. L. Ogleby
School of Geomatics,
The University of Melbourne,
3010, Victoria, Australia,

T. Tanijiri
Medic Engineering,
Kyoto, Japan
http://www.rugle.co.jp/

M. Yoshino
National Research Institute of Police Science,
Chiba, Japan
http://www.nrips.go.jp/index-e.html

Introduction

Problems with human bite mark analysis

Bite mark analysis is currently contentious. For a subject with such potentially serious outcomes for both suspect and victim, little research analysing methods and evaluating outcomes has reached peer reviewed journals [1]. Although admissibility of bite mark evidence has been established and routinely accepted in the USA and other legal systems for a long time [2] some odontologists argue that bite mark methodology has never undergone critical evaluation and legitimately passed the Frye [3] test for admissibility. This problem is also relevant for other areas such as earprint identification [4]. Other legal observers are concerned that forensic odontologists are giving insufficient critical attention to the quality of bite mark evidence presented to the courts [5, 6]. Central to the problem of analysis is the difficulty of comparing 2-dimensional images of a bite mark with 3-dimensional replicas of dentitions which may have caused them.

Over time, a deficiency in quantitative bite mark research has resulted in uncertainty in bite mark evidence in legal systems worldwide, particularly in Australia. The natural tendency to see what one wants to see, thereby tempting examiners to over-interpret bite mark evidence, has led to serious difficulties when bringing such evidence before the courts [7]. This area of forensic science requires standardisation to ensure consistency of expert opinions. Two notorious Australian cases [8, 9] have seen bite mark evidence rejected as unsafe, and convictions overturned on

appeal. Perhaps for such reasons, bite mark analysis is currently undergoing review. In general, courts now look for quantitative rather than simply descriptive analysis before accepting scientific evidence. It can be anticipated that future developments in the analysis of bite marks will need to follow this general trend if convictions are going to be made with confidence.

Importance of the third dimension

Many studies have described and quantified bite patterns in two dimensions (photographs, overlays etc.). Yet, despite the fact that the dentition of the biter and the corresponding bite marks are both 3-D phenomena, there have been few 3-D analyses [10–12]. This is surprising, but it may reflect the lack of access to methods of measuring in three dimensions that have recently become available. Legal problems involving bite mark evidence suggest that alternative methods of analysis may be required, and the logical first step is to analyse bite marks in 3-D.

There are three factors of 3-dimensionality involved when one person bites another: the curvature of the skin, the shape of the biting dentition and the depth of the injury should the tooth/teeth puncture the skin to create a depression, although this is infrequent. The injury, as it is being inflicted, is a 3-dimensional event—the skin deforms to accommodate the shape of the teeth. However, once the teeth are withdrawn, the skin is restored near to its original shape and the resultant mark is represented without depth information on the curved surface of the skin. If the force of the bite is great enough to leave an indentation in the skin, then the mark is also 3-dimensional. Injuries range from a defined mark/s, a diffuse bruise, complete removal of tissue and swelling due to inflammation.

Aim of study

This study develops a method for 3-D imaging and quantitative comparison of human dentitions and the corresponding simulated bite marks. This study also defines an optimum threshold for this sample, which segregates matches from non-matches.

Materials and methods

Study models and simulated bite marks

Forty two third year students from the School of Dental Science, The University of Melbourne, Australia, contributed a maxillary and a mandibular dental-stone study model of their own teeth. Students were then asked to bite into a wafer of double-thickness, pre-heated acrylic dental wax (Lordell Trading Pty Ltd, Wetherill Park, New South Wales, Australia) to create an upper and lower bite impression of their own teeth. These impressions were called *simulated* bite marks as they were made in wax and not human skin. Dental wax has been used previously in bite mark research [13, 14] and during bite mark investigations. Corresponding sets of models and wax bites were numerically labelled; all upper dentitions and bite models were labelled ‘U’ and lower dentitions and bite models ‘L’.

Reverse models of wax bite impressions

Mirrored or reverse models of the wax bite impressions were created to make the laser scanning process faster and more efficient. Imaging an indentation, i.e. a bite in wax, would be difficult. The alternative process of scanning an outward protruding surface would result in obtaining the maximum amount of data points. The substrate selected to create the reverse models was type 3 low viscosity Hydroflex hydrophilic vinyl polysiloxane impression material (GC Corporation, Tokyo, Japan), the physical properties of which are suitable for this purpose. It remains highly stable after setting, can be stored long-term without shrinking or decomposing and has 99.7% recovery from deformation. Hydroflex has an accuracy of 20±4 μm and meets the ISO 4823 International Standard [15] and ADA Specification No.19 [16].

The models were made by squeezing the impression medium and catalyst simultaneously from a two-chambered, triggered dispenser onto the wax bite. Latex gloves were not worn as research suggests that they cause retardation in the setting time of some vinyl polysiloxane materials [17]. Hydroflex was applied on one side of the wax sheet and was allowed to flow under the force of gravity to force out air bubbles. Setting time was approximately 30 min depending on room temperature and humidity. Once set, the Hydroflex was lifted out of the wax resulting in a reverse bite model of around 5-mm thickness. The process was repeated for the opposite side of the wax. Labelling was achieved by engraving the wax with a mirrored number so the label could be read sequentially once the Hydroflex was lifted from the wax.

Laser scanning equipment

The FARO Gold Arm (2001 FARO Technologies Inc, Lake Mary, FL, USA) and ModelMaker H40 [3-D Scanners (UK) Ltd, Coventry, UK] (Fig. 1a) were used in conjunction to laser-scan the study models and bite models (Fig. 1b) to create 3-D images.

The FARO Arm (http://www.faro.com, 8 Aug 2001) is a highly accurate measurement instrument designed for use in engineering and manufacturing for the control of dimensional quality in mass production. The arm can be screwed or fixed with clamps to a flat surface, which requires a high degree of stability to achieve the best results. The Gold Arm, with an accuracy of ±84 μm, was used in this project. The arm portion of the instrument is composed of two shafts of lightweight aircraft-grade aluminium, internally counterbalanced for ease of use. Rotation of the

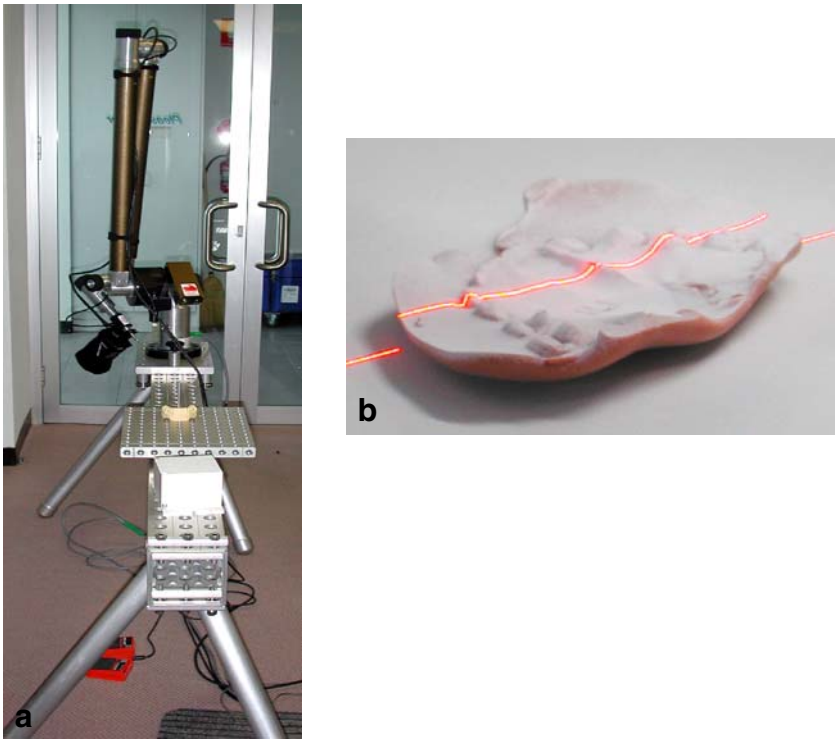

Fig. 1 **a** The FARO Gold Arm and ModelMaker H40 laser scanner used to digitise the study dentitions and Hydroflex bite models and **b** a laser line generated by the ModelMaker passing over the surface of a bite model. The image is reflected back into the ModelMaker's camera to create the resultant 3-D data set

shafts about seven pivot points provides a spherical working space 3 m in diameter.

The ModelMaker H40 (http://www.3dscanners.com, 8 Aug 2001) is a hand-held, non-contact reverse engineering and inspection sensor which mounts to the end of the FARO Arm. The scanning system works on the principle of laser stripe triangulation. A laser diode and stripe generator projects a laser line onto the object to be scanned. The line is viewed at an angle by a camera, and height variations in the object are seen as changes in the shape of the line. The resulting captured image of the stripe is a profile that contains the shape of the object. The accompanying surfa board uses digital signal processing to convert video data to digital data to capture surface shape in real time at over 14,000 points per second. Either keyboard and mouse, or a foot pedal, drives the system.

Pre-scan preparation

The matt, beige surface of the dental stone study models was ideal for scanning; however the shiny surface of the Hydroflex models was too reflective. Each Hydroflex model was sprayed with Flawcheck visible inspection system [DY-MARK (Aust) Pty Ltd, Laverton North, Victoria, Australia], a fine white powder which gave the surface a matt finish assisting the camera in detecting maximum laser signal. The thickness of sprayed powder was sufficient to reduce the surface shine of the Hydroflex. One pass of the spray results in a layer of approximate thickness 10–30 μm according to J. Morgan of DY-MARK (Aust) Pty Ltd (personal communication, 2 June, 2005). Therefore, the effect of this additional coating is minimal.

Laser scanning process

The system was calibrated against a machined alignment cube of precisely known dimensions. The calibration cube was also used as a pedestal to elevate the models for easier scanning. It was essential that the position of the model remained undisturbed during scanning, otherwise the system would reassign the location of the object in space and a double-image would result. If the model was displaced, the process would need to be repeated from the start.

A pre-scan was initially taken by passing the laser line over the model in several directions so the system registered the size and location of the object in space. The colour of the resultant 3-D image was white and composed of thousands of interlinked polygons (Fig. 2). A systematic method for scanning each study model was developed: first, the facial aspect, followed by the occlusal and then the lingual surfaces. Being systematic was important to avoid overlapping passes of the laser line, as patches of data accumulated on top of one another creating a ruffled effect once the polygons had been merged. Using the lasso tool to select small areas reduced overlapping, as new data was added to the selected areas only. Scanning time was approximately 30 min for a complete set of study models and 15 min for a set of the less undulating Hydroflex models.

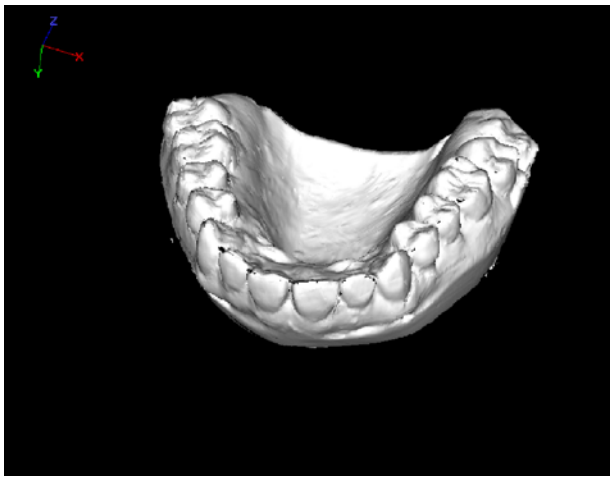

Fig. 2 3-D image of a maxillary study model as a result of laser scanning. Thousands of interlinked polygons represent the morphology of the dentition

Data processing

Images were processed using ModelMaker software (Version 3.3.3.3 1996–1998 3D Scanners UK Ltd, Coventry, UK) by following a sequence of steps. Superfluous data were 'cleaned' or deleted from around each image, for example the data from scanning the cube underneath the model. Groups of data points or polygons that compose each image were 'merged' or linked. Small holes or areas void of data between scan patches were 'filled' to produce a continuous surface. Hole size ranged from 50 to 500 points, and considering that a scan of each half of a study model was approximately 140,000 points, the effect of extrapolating the data for these holes was not detrimental to the anatomical accuracy of the surface. A minimum amount of 'smoothing' was done for each image to counteract any ruffling effect caused by overlapping passes of the laser. Images were decimated to between 15 and 25 MB and converted to stereolithography interface format (stl) files to enable viewing in 3D Rugle3 software (Version 1.0 1998–2001, Medic Engineering Corporation, Kyoto, Japan. Release 24.09.2001 Australia).

3D Rugle3 software

3D Rugle3 (http://www.rugle.co.jp, 5 Jun 2001) is a 3-D data viewing and measurement software program used predominantly in research on 3-D facial analysis [18, 19]. The program is composed of five modules—superimposition, basic measurement, intersurface distance, fitting and simulation. The intersurface distance and basic measurement modules were used in this study.

The 3-D images of the dentitions and bite marks were imported as stl files into the intersurface distance module. Four points—the midpoint of the buccal cusp of each of the second pre-molars and the midpoint of the occlusal surface of each of the anterior incisors—were designated on each image using the 'correct tilt' function to align the image with the x–y plane, the x-axis and the midline. This resulted in a standard orientation of each image. The image was exported into the basic measurement module as a materials and geometry format (mgf) file. Mgf files are smaller than stl files, therefore, they are easier and faster to manipulate using the software. Small voids or holes in the data, which are often caused by the process of decimation, were filled using the 'filter, fill hole' function. Holes in the data are filled using height or z values of the surrounding pixels, and the original data set is not affected.

Morphometric landmarks

The first five teeth of each quadrant (incisors, canines and pre-molars) were used for landmark placement. Molar teeth are less likely to make contact with the skin during a bite due to their posterior location within the oral cavity. Several dentitions in the sample had pre-molar teeth missing and the molars had moved anteriorly to fill the gap. The molar was included in these cases. Landmarks were placed on the buccal cusps of pre-molars and molars.

A total of 42 landmarks were placed on each image, 30 on the teeth and the remainder along the midline and reference line (Fig. 3). The reference line joins the peak points of the second pre-molars and the midline joins the midpoint of the reference line and the midpoint between the anterior incisors. Landmarks 1–30 were placed on the occlusal surface of each tooth and consisted of the peak point, the mesial-most point and the distal-most point. 3D Rugle3's 'max point' function allowed objective placement of the peak point on each tooth by locating the highest z value within a defined area. The operator located the mesial-most and distal-most points. Landmark 31 was the midpoint of the reference line, landmark 32 was the midpoint between the anterior incisors and landmarks 33–42 were placed along the midline. Lines were drawn from the distal-most point of each tooth to the midline, and landmarks were placed at the intersection each line made with the midline.

Statistical analysis

A number of variables comprising curves, angles and distances were created using the x, y, z co-ordinates of each

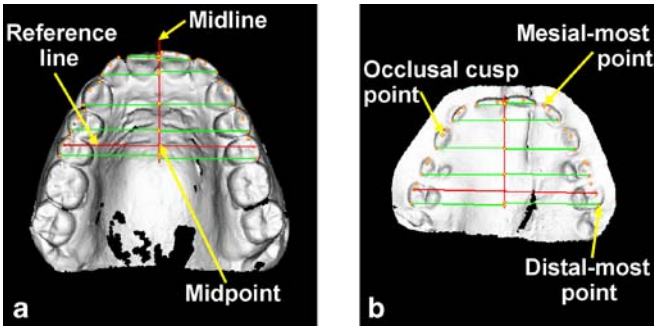

Fig. 3 Forty-two landmarks were placed on the 3-D images of each **a** study model and its **b** corresponding Hydroflex bite model

landmark providing a numerical description of the dentitions and bite marks. Variables underwent transformations such as square root and logarithm, to approximate symmetry and normality, since discrimination is likely to be more effective using variables with these properties. The variables are as follows:

1) Curve of the arch defined by landmarks 1–30:

$$y_i = a_1 x_i^2 + a_2 x_i^4$$

y_i = transformed y-value; x_i = transformed x-value; a_1, a_2=coefficients of the curve; i=1, 2,..., 30

2) From this curve, the point with the smallest residual (distance from the curve in the y direction) and the point with the largest residual generated the variables: minres and maxres.
3) Length of each tooth (mesial-most point to distal-most point)

$$l_j = \sqrt{\left(x_{3_{j-2}} - x_{3_j}\right)^2 + \left(y_{3_{j-2}} - y_{3_j}\right)^2}$$

for j=1,⋯,10 together with the 'total length'=$\sum_{j=1}^{10} l_j$

4) Nine distances (point 2 to each peak point):

$$r_k = \sqrt{\left(x_2 - x_{3k+2}\right)^2 + \left(y_2 - y_{3k+2}\right)^2}, k = 1, \ldots, 9$$

5) Nine angles (formed by 'point 2 to each peak point' and the 'midline')

$$a_k = \tan^{-1}\left(\frac{x_2 - x_{3k+2}}{y_2 - y_{3k+2}}\right), k = 1, \ldots, 9$$

A matrix was created to compare all possible combinations of matches and non-matches of dentitions and bite models. For each combination, the absolute differences between the variables in the dentition and the same variables in the bite model were recorded. These absolute differences reflect the quantitative proximity between the dentition and the bite model with which it is compared. The matrix consisted of 1,722 combinations: 42 dentitions × 41 bite models. The sample was composed as follows: 40 complete sets of dentitions and their corresponding Hydroflex bite models, resulting in 40×40=1,600 combinations for each set, 40 of which were true matches. That is, dentition 1 matches bite model 1 but does not match the remaining bite models 2–40; dentition 2 matches bite model 2 but does match bite model 1 or 3–40, etc. Two additional dentitions were included for which the bite model data was excluded, and one bite model for which the dentition data was excluded. Hence, the total of 1,722 combinations came from 42 dentitions and 41 bite models (40 matches, 1,682 non-matches).

Logistic regression was used to obtain a predictive model, or algorithm, for a match (available from author on request). Cross-validation was also implemented on the data; in turn, each bite model was removed from the data set and a logistic regression model was fitted using the rest of the data. The fitted statistical model was then used to make predictions for the 41 combinations in the omitted data. This process was repeated for each of the 42 dentitions. In this way, the data used to make predictions was separate from the data used to estimate the performance of the algorithm in all cases, which gives unbiased estimates of sensitivity and specificity. Alternatively, when cross-validation is not used, the data used to test the predictive power of the algorithm are the same as those used to generate it, which tends to give over-estimates of the algorithm's predictive performance.

The probabilities generated were expressed as values for sensitivity and specificity:

- Sensitivity=P(TP)=1−P(FN)
- Specificity=P(TN)=1−P(FP)

where P(TP)=Probability of a true positive=probability of obtaining a match for dentitions and bites that do in fact match; P(TN)=Probability of a true negative=probability of obtaining a non-match for dentitions and bites that do not in fact match; P(FP)=Probability of a false positive=probability of obtaining a match for dentitions and bites that do not in fact match; P(FN)=Probability of a false negative=probability of a non-match for dentitions and bites that do in fact match.

These probabilities were expressed in an ROC curve, a graphical representation of the compromise between the true positive (TP) and false positive (FP) probabilities for every possible threshold value [20]. The ROC graph allows a continuous assessment of the relationship between P(TP) and P(FP) for each threshold value and incorporates a degree of uncertainty in the decision-making, rather than simply making a dichotomous, yes or no decision [21]. ROC curves are typically used in medicine and are useful aids in the diagnosis of disease, such as human immunodeficiency virus or cancer. ROC analysis has been used previously in bite mark analysis [22, 23].

An ideal ROC curve (Fig. 4a) would be a line which followed the y-axis and made a right angle following the line extending horizontally from (0, 100). The optimal point on this line would be at (0, 100) where the probability of obtaining a true positive was 100% and a false positive 0%. Other points along the curve represent a range of values for true and false positive rates. It is unlikely that any realistic situation would result in an ideal ROC curve, so a compromise between TP and FP rates must be achieved.

Figure 4b depicts a partial ROC curve for the dentitions and bite marks used in this study and Table 1 shows how the TP and FP rates vary for several threshold values on either side of the optimum threshold for this curve. For example, at threshold 0.18, the TP rate or the probability that a dentition and bite model were correctly identified as a match, is only 55% which results in a FP rate of 3%. Such a low false positive rate is almost ideal, however, the sensitivity should be higher. At the other end of the scale at

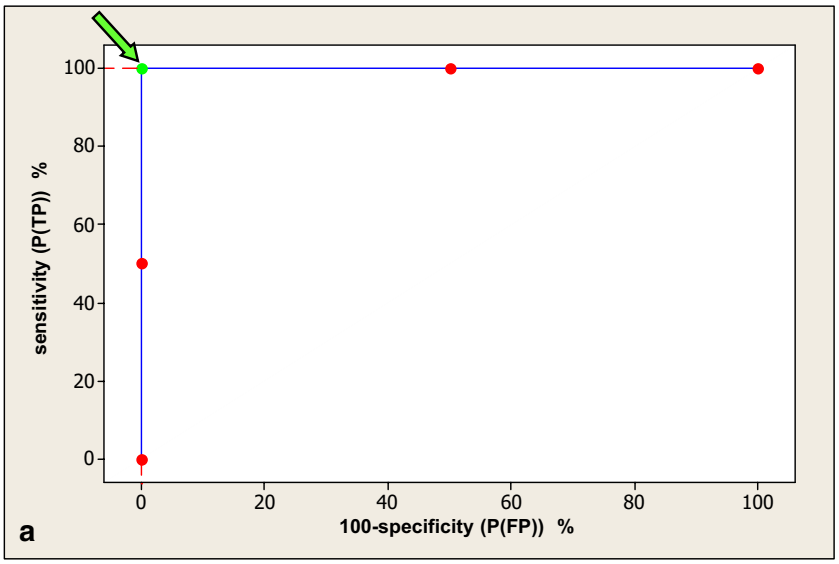

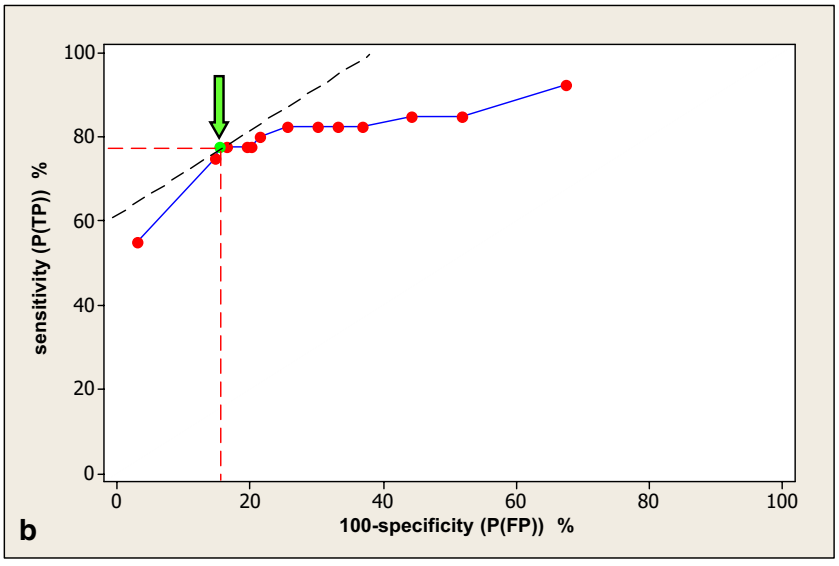

Fig. 4 A receiver operating characteristic (ROC) graph was used to illustrate the data. **a** Shows an ideal ROC curve and **b** a partial ROC curve for this sample using cross-validated data. The optimal points for each graph are arrowed

threshold 0.006, the TP rate is much higher which is good, but at the expense of the FP rate which is now 26%. The best point on the graph is a compromise between TP and FP rates.

Table 1 The relationship between threshold, the probability of a true positive P(TP) and a false positive P(FP) for the partial ROC curve (Fig. 4b). The optimal values are in boldface

Threshold	Sensitivity P(TP)%	1-Specificity P(FP)%
0.006	82.5	25.6
0.01	80.0	21.4
0.011	77.5	20.2
0.012	77.5	19.6
0.016	77.5	16.5
0.018	**77.5**	**15.4**
0.02	75.0	14.7
0.18	55.0	3.0

The optimal point (arrowed) in Fig. 4b is one with the least distance from the top left corner where the threshold value is 0.018. At this point the TP rate is 78% and FP rate 15%. At this point, the TP rate is as high as it can be without consequently causing the FP rate to be too high. Therefore, at the optimal point on the ROC curve for this sample, **15% of non-matching dentitions and bite models could not be distinguished from the true match** (i.e. a 15% chance of wrongly convicting an innocent person). Whilst 78% of matching dentitions and bite models were correctly identified as a match by the algorithm.

An ideal situation for this sample would be 42 true matches (TP rate=100%) and the remaining combinations would not match. However, the actual situation for this sample was:

- Only four matched with self (i.e. true match) and no other
- Twenty-seven matched with self and at least one other
- Seven did not match with self but matched with others

Table 2 The first ten (out of 296) combinations of dentitions and bite models with a threshold value ≥0.018, and therefore considered a match

Dentition	Bite model	Threshold
43	43	0.933
8	1	0.885
4	4	0.872
4	44	0.847
85	8	0.793
30	30	0.788
1	1	0.747
52	52	0.737
4	52	0.715
3	3	0.688

Labelling of models was not consecutive for a number of reasons, hence model numbers such as 43, 85 and 52. However, be assured that they formed part of the 42 models used in this study

– Four did not match with anything, including self

When the matrix was sorted according to threshold value and the combinations ranked according to this value, the first 296 combinations had a threshold value ≥0.018, so were considered a match. The first ten are listed in Table 2 as an example. The dentition model labelled 43 and its corresponding bite model, having the highest threshold value, were the closest match as determined by the algorithm.

Image visualisation and animation

Images were imported into 3D Rugle3 software for visualisation. During scanning, each data point was represented by an *x*, *y* and *z* Cartesian co-ordinate and images could consequently be rotated and viewed from any angle. A selection of the images were imported into 3ds Max [Discreet (Autodesk) release 4.0 commercial 2001] animation software and rendered in artificial colours. Animations were created from (1) a positively matched dentition and bite mark showing near perfect registration, (2) a non-matching dentition and bite mark, (3) a cutting plane to illustrate topography of biting surfaces of teeth, (4) a maxillary dentition registering with an ink bite printed onto skin. These animations can be viewed on http://www.dent.unimelb.edu.au/3dbitemarks/.

Discussion

Although the morphology of each dentition in this study may be unique, we hypothesised that very similar and indeed *indistinguishable* bite marks may be produced by *a number* of different dentitions, despite the uniqueness of these dentitions. Bite marks produced by different dentitions in a firm substrate, cheese for example, may be more unique with respect to each other, and more similar to their corresponding dentitions, than bite marks inflicted by the same set of dentitions on a highly deformable substrate, like skin. Dynamic, tissue and postural distortion, as explained by Sheasby and MacDonald [24], have a significant impact on the quality of a bite mark on skin.

The results of this study indicated that 15% of combinations of dentitions and bite models in this sample were categorised as a match when they were in fact a non-match, i.e. 15% of non-matching combinations were indistinguishable from the true match. This translates to six out of the 42 people in this sample at risk of being false positives, or wrongly convicted. This figure is only indicative of this particular sample and may be lower in actual casework, but this is not certain.

Study sample

Some may criticise the sample used in this study. Study models of the dentition were obtained from a group of young, university students and may provide an unusually homogenous sample. A number of subjects may have undergone orthodontic treatment, a convergent process resulting in different people having teeth similarly arranged. It is consequently possible that there is a higher degree of similarity amongst dentitions in this sample compared with a sample of high forensic significance, i.e. the sample may not be typically representative of dentitions commonly examined in the wider community, which may exhibit more uniquely identifying features such as missing or fractured teeth. Dentitions in this sample exhibited a low number of uniquely identifying characteristics, influenced perhaps by the young age (early 20's) of the subjects, the good condition of their teeth and their socio-economic background. However, even with a more varied sample, the possibility still exists that a number of people may have dentitions similar enough to produce indistinguishable bite marks.

Wax as an impression medium

Wax was chosen as a bite impression substrate because it is a slightly imperfect recorder of tooth shape, as is human skin. However, we acknowledge that no alternative substrate can accurately mimic the complex physical mechanics of human skin.

Error

The process of producing reverse bite models from the wax bites and creating a digital image by laser scanning would have introduced a certain amount of error. However, Hydroflex, with an accuracy of 20±4 μm, was the best material to use to minimise this error. Acrylic wax is easily deformed with heat and force, so it was advantageous to replace the wax bites with more robust Hydroflex models. Also, laser scanning with minimal overlapping of scan patches was the best method to keep error to a minimum.

Laser scanning

Use of the laser scanner and associated equipment required a certain degree of training, and technique improved with practice. Before starting to scan the study samples, the operators practised using the equipment on a dental model that was not included in the study.

Best scanning results were achieved by using minimum passes of the laser to reduce the ruffling effect from overlapping of scan patches. The scanner had difficulty detecting sharp edges, in particular the incisal edges of the anterior incisors, so it was important not to over-scan these edges as the data may provide a false representation of the morphology of the tooth.

Image processing

There is a conflict between decimating images enough to produce files sufficiently small to open and manage in viewing software; however, if one over-decimates too much data can be lost. It is important to get the crispest, cleanest original laser scanned image possible in the first instance. If there is too much 'noise' or excess data present in the original scan, this will give an inaccurate surface representation and it is wiser to re-scan the model. For this reason, the corresponding images of two dentitions and one bite model used in this study were excluded. The images were of insufficient quality to accurately represent the true morphology and would require re-scanning.

Landmark placement

The peak point of the occlusal surface, or the part of the tooth with the greatest distance from the gingiva, was chosen rather than the midpoint, as this is the first point of contact with the skin during a bite.

Animation

The use of 3ds Max requires some expertise and the process of creating an animation is time-consuming, however the results can be impressive. Such a pictorial display may be of benefit in a courtroom situation to assist the jury in understanding evidence, not only with bite mark analysis but in many other fields. 3-D crime scene reconstruction is currently used for training and in court in two Australian states, Queensland and Western Australia, and has been beneficial (http://www.qmisolutions.com.au/article.asp?aid=77&pfid=5, 15 Nov 2005).

3-D in the future

It is expected that 3-D imaging equipment will become more affordable and accessible in the future. If 3-D imaging and quantification techniques were developed and were proven to be successful, police and forensic investigation institutions would be more encouraged to utilise funds in this area.

Summary

The ideas and methods developed in this study for 3-D imaging and quantitative comparison of human dentitions and their corresponding bite marks are by no means a final solution to the complex problems bite mark analysis presents. We hope this research will increase awareness about the possibility that the number of false positives resulting from bite mark evidence given in court may be higher than we realise, a problem which is not unique to bite mark analysis but affects many other areas of forensic science such as earprint identification (http://www.forensic-evidence.com/site/ID/DNAdisputesEarlID.html, 15 Sept 2005). We hope researchers will be inspired to continue to investigate the 3-dimensionality of bite marks and to improve the science of bite mark analysis.

Acknowledgements We are grateful for the advice and generous assistance of the participants of the study; Scanning and Inspection Pty Ltd, Melbourne; the Victorian Institute of Forensic Medicine, Melbourne; Mr David Thomas and Mr Ronn Taylor, School of Dental Science, The University of Melbourne, Australia and Mr Chris Scott. We are grateful for the financial support of the Australian Academy of Forensic Sciences, the Australian Dental Research Foundation and The University of Melbourne.

References

1. Pretty IA, D Sweet (2001) The scientific basis for human bitemark analyses—a critical review. Sci Justice 41:85–92
2. People v. Marx, in 54 Cal. App. 3d 100, 126 Cal Rptr. 350. 1975
3. Frye v. United States, in 293 F.1013 (D.C. Circ). 1923
4. Rutty GN, Abbas A, Crossling D (2005) Could earprint identification be computerized? An illustrated proof of concept paper. Int J Legal Med, on-line publication 10.1007/s00414-005-0527-y
5. Rothwell BR (1995) Bite marks in forensic dentistry: a review of legal, scientific issues. J Am Dent Assoc 126:223–232
6. Gundelach A (1989) Lawyers' reasoning and scientific proof: a cautionary tale in forensic odontology. J Forensic Odontostomatol 7:11–16
7. Wells D (1998) Bitemarks (Teaching resource material for Forensic Diploma of Clinical Forensic Medicine). Monash University, Victoria, Australia
8. Raymond John Carroll, in Australian Criminal Reports (1985) Court of Criminal Appeal, Queensland, p 410
9. Lewis v The Queen, in Federal Law Reports (1987) Court of Appeal of the Northern Territory, p 104
10. Forrest A, Davies I (2001) Bite marks on trial—the Carroll case. Aust Soc Forensic Dentistry 18:6–8
11. Thali MJ, Braun M, Markwalder ThH, Brueschweiler W, Zollinger U, Malik NJ, Yen K, Dirnhofer R (2003) Bite mark documentation and analysis: the forensic 3D/CAD supported photogrammetry approach. Forensic Sci Int 135:115–121
12. Martin-de las Heras S, Valenzuela A, Ogayar C, Valverde AJ, Torres JC (2005) Computer-based production of comparison overlays from 3D-scanned dental casts for bite mark analysis. J Forensic Sci 50:127–133

13. Nambiar P, Bridges TE, Brown KA (1995) Quantitative forensic evaluation of bite marks with the aid of a shape analysis computer program: Part 1; The development of "SCIP" and the similarity index. J Forensic Odontostomatol 13:18–25
14. Sweet D, Bowers CM (1998) Accuracy of bite mark overlays: a comparison of five common methods to produce exemplars from a suspect's dentition. J Forensic Sci 43:362–367
15. International Standard Organisation (ISO). Dental elastomeric impression materials, ISO 4823, 2nd edn. 1992-03-15, Section 5.11 Detailed reproduction, p 2
16. Revised American Dental Association specification No.19 for non-aqueous, elastomeric dental impression materials (1977) J Am Dent Assoc 94:733–741
17. Baumann MA (1995) The influence of dental gloves on the setting of impression materials. Br Dent J 179:130–135
18. Fraser N, Yoshino M, Imaizumi K, Blackwell SA, Thomas CD, Clement JG (2003) A Japanese computer-assisted facial identification system successfully identifies non-Japanese faces. Forensic Sci Int 135:122–128
19. Yip E, Smith A, Yoshino M (2004) Volumetric evaluation of facial swelling utilizing a 3-D range camera. Int J Oral Maxillofac Surg 33:179–182
20. Swets JA, Dawes RM, Monahan J (2000) Psychological science can improve diagnostic decisions. Am Psychol Soc 1:1–26
21. Pretty IA (2005) Reliability of bitemark evidence. In: Dorion RBJ (ed) Bitemark evidence. Marcel Dekker, New York, pp531–545
22. Whittaker DK, Brickley MR, Evans L (1998) A comparison of the ability of experts and non-experts to differentiate between adult and child human bite marks using receiver operating characteristic (ROC) analysis. Forensic Sci Int 92:11–20
23. Pretty IA, Sweet D (2001) Digital bite mark overlays—an analysis of effectiveness. J Forensic Sci 46:1385–1391
24. Sheasby DR, MacDonald DG (2001) A forensic classification of distortion in human bite marks. Forensic Sci Int 122 (1):75–78